A Closed-Loop Recycling Technology for γ-TiAl from Precision Cast Low Pressure Turbine Blades

Peter Spiess[1,*], Marek Bartosinski[1], Todor Stoyanov[2], Julio Aguilar[2], and Bernd Friedrich[1]

DOI: 10.1002/cite.201500063

Due to the high generation of scrap in the process chain of γ-TiAl semi-finished goods and products, a suitable recycling process shows great potential to reduce production costs. Based on this circumstance, a closed loop recycling process for titanium-aluminide scraps was developed. Resulting from this process, as a significant innovation for the titanium industry, it is possible to recycle titanium-aluminide scraps and produce material with minimal oxygen content and almost no observable difference to primary alloys.

Keywords: Investment casting, Low pressure turbine blade, Recycling, TiAl

Received: July 02, 2015; *accepted:* August 31, 2015

1 Introduction

In 2008, the global CO_2 emissions generated by aviation were indicated by Clemens [1] with a new all-time high of over 650 mio. t a^{-1} already. Since Boeing forecasts a rapidly increasing global transport capacity with an annual 5 % growth of revenue passenger kilometers (RPK) in the next 25 years, the necessity of the substitution of heavy superalloys by structural intermetallic alloys to soften the likewise increasing production of pollutant emissions as well as fuel consumption is given. In spite of their high price and in particular the high production costs of semi-finished products the group of preferred intermetallic alloys include the γ-Titaniumaluminides, which are characterized by eminent properties like high specific elasticity modulus, high melting point (about 1450 °C), low density (3.9 – 4.1 g cm^{-3}), high specific creep resistance (39 – 46 GPa $cm^3 g^{-1}$) and good oxidation resistance in subset temperature ranges [1 – 3].

The most common processing of γ-Titaniumaluminides consists of the very expensive double or triple remelting in a vacuum arc furnace (VAR) of afore pressed electrodes of primary materials. By the use of a subsequent spin-casting process so called "master heads" are produced. They are used in investment casting processes where a not inconsiderable amount of the material solidifies in runners and feeders of the casting system or as a skull in the crucible and is obtained as scrap. Furthermore, the fabrication of the semi-finished products is performed under a low material utilization which results in an extremely high "buy-to-fly" (BTF) ratio often exceeding 20 [4]. Due to this high generation of scrap in the production process; a suitable recycling process shows great potential to reduce production costs. Based on this circumstance; IME Process Metallurgy and Metal Recycling (IME) developed a closed loop recycling process for titanium-aluminide scraps. Extensive research on the individual process steps has already been carried out and was published by Stoephasius [5], Lochbichler [6] and Reitz [7]. In cooperation with ACCESS Technology (ACCESS) it was now possible to evaluate the entire process from scrap material to finished precision cast low pressure turbine (LPT) blades.

2 Background

2.1 TiAl Recycling Principles

While processing titanium and its alloys, the main obstacle is formed by the strong affinity to oxygen. Furthermore, the oxygen solubility in titanium can reach values over 30 at % O (Fig. 1) without forming oxide phase segregations. Since the material properties like ductility are highly affected by the presence of oxygen, liquid titanium has to be handled with care and all melting processes require a controlled inertgas atmosphere.

In matters of scrap composition and shape, using vacuum induction melting (VIM) as initial consolidation step results in a very high process flexibility. Furthermore, VIM offers the possibility of online sampling and composition corrections. In comparison to commercial pure titanium, Lochbichler [6] shows a remarkably decreased titanium activity in TiAl alloys (Tab. 1). Nevertheless, while using alumina crucibles for VIM of TiAl, an oxygen pickup of 5000 ppm

[1]Peter Spiess, Marek Bartosinski, Prof. Dr. Dr. h.c. Bernd Friedrich, IME Process Metallurgy and Metal Recycling, RWTH Aachen University, Intzestraße 3, 52056 Aachen, Germany; [2]Todor Stoyanov, Dr. Julio Aguilar, ACCESS Technology GmbH, Jülicher Straße 322, 52070 Aachen, Germany.

 © 2015 WILEY-VCH Verlag GmbH & Co. KGaA, Weinheim

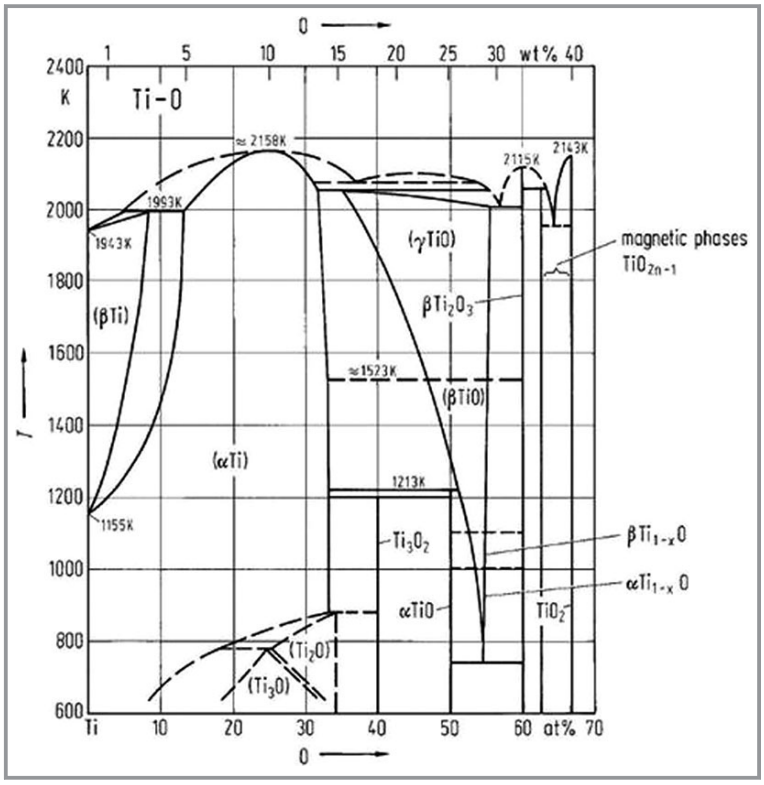

Figure 1. O-Ti phase diagram [8].

Table 1. Titanium activities and liquids temperatures of chosen Ti-bearing alloys (Data: FactSage, ELEM).

Alloy	T_{Liq} [°C]	a_{Ti}
cp Ti	1668	~1
TiAl6V4 [mass %]	1686	0.87
FeTi70 [mass %]	1109	0.56
TiAl50 [at %]	1517	0.24
FeTi30 [mass %]	1433	0.07

can be observed which exceeds the specs of approx. 1200 ppm by far.

In general, oxide or non-oxide-based refractories feature a significantly higher solidus temperature than that of the processed alloy, a sufficient thermochemical stability against it, and almost no addiction for volatilization at high temperatures. These mentioned attributes can be expressed by the standard Gibbs free energy of refractories. Consequently, the chemical stability of oxide and non-oxide refractories against titanium can be grossly classified. An increase in temperature leads to a dramatic reduction of the thermochemical stability of oxides and non-oxides (except B_4C, SiC and TiC). With regard to non-oxides, TiC and TiN represent the most stable phases, i.e., titanium possesses the highest affinity to C and N at all. By calculating the oxides' standard Gibbs free energy, only CaO, Y_2O_3 and ZrO_2 have been identified as sufficiently stable against titanium. The most stable oxide can be named as CaO while it is also the best choice in terms of costs. The main disadvantage when using pure lime is its hygroscopic nature. Therefore, the lime crucibles have to be handled with care. Another handicap is the combination of high temperatures and low pressures during VIM. The consequence is the dissolution of lime as Ca and O in the melt. As a result of its high vapor pressure, an evaporation of metallic calcium takes place which condenses at the water cooled furnace chamber. Hence, the reactions' thermochemical equilibrium cannot be reached which results in continuous dissolution of CaO and subsequent oxygen enrichment in the melt. The main influence on the reaction speed of the dissolution steps is the temperature.

Via charging of alloying elements or reacting agents, i.e., deoxidation agents, it is possible to influence the melt chemistry during vacuum induction melting. The idea is the introduction of $CaAl_2$ (when using lime crucibles) or metallic Y (when using yttria crucibles) as deoxidation agents to achieve the following reactions (Eq. (1)–(3)):

$$[TiO]_{TiAl} + [Ca]_{TiAl} = \langle CaO \rangle + Ti \quad (1)$$

$$[TiO]_{TiAl} + \{Ca\} = \langle CaO \rangle + Ti \quad (2)$$

$$3\,[TiO]_{TiAl} + 2\,[Y]_{TiAl} = \langle Y_2O_3 \rangle + 3\,Ti \quad (3)$$

where < > stands for solid, [ ] for dissolved, and { } for gaseous compounds.

Experiments show a sufficient deoxidation of TiAl to values below 700 ppm O when using $CaAl_2$. Unfortunately, a simultaneous formation and precipitation of $Al_2O_3{\cdot}CaO$ spinel is favored. The application of Y metal as deoxidant to TiAl has not succeeded. This can be explained by the higher solubility product of Y_2O_3 in comparison to CaO in the melt. The thermochemical calculations of the Ca-O and Y-O equilibria in TiAl melts as a function of temperature are shown in Fig. 2. Oxygen and calcium pickup in TiAl is much lower when melting in CaO crucibles than applying Y_2O_3 (i.e., Y and O) as refractory. Dissolution of CaO leads to oxygen concentrations of 2600 ppm on average versus 3100 ppm utilizing Y_2O_3 (without deoxidation). For compensation of Al-losses due to the low operating pressures, a higher amount of aluminum can be charged from the start.

For final deoxidation of titanium aluminides, the electroslag remelting (ESR) process can be applied as an intermediate step of the recycling process. Since the vapor pressure of Calcium is very high, the deoxidation step of Ti and Ti alloys by metallic calcium at typical VIM operating pres-

 © 2015 WILEY-VCH Verlag GmbH & Co. KGaA, Weinheim

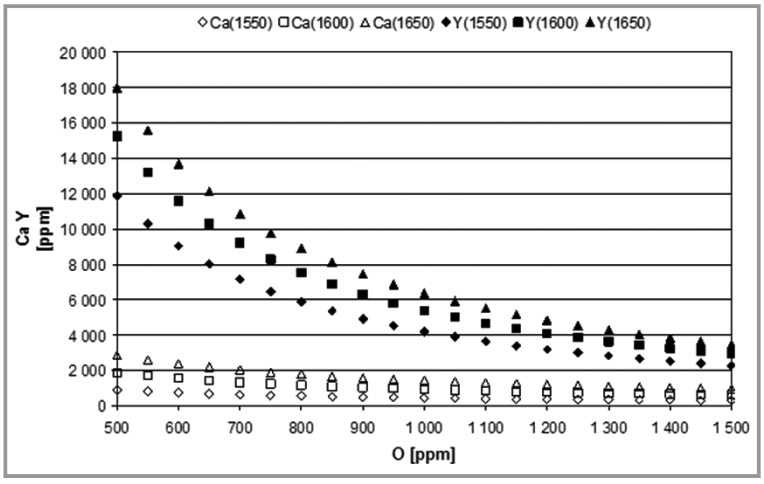

Figure 2. Dissolved Ca and Y in CaO and Y_2O_3 saturated liquid TiAl versus dissolved oxygen at three different temperatures. Note: $a(CaO)a(Y_2O_3) = 1$ [6, 9, 10].

sures (~0.8 bar) is not feasible experimentally. Thus, the final deoxidation step is conducted under pressure to prevent violent Ca losses from the slag. For remelting, CaF_2-based slags exhibit the best combination of thermochemical stability, stable processing conditions final ingot quality and availability [11]. Due to its good solubility in the slag, high oxygen affinity and availability of experimental datasets for Ca-O equilibria in titanium melts, calcium is chosen as a reactant. Based on thermochemical calculations of the CaF_2-CaO-Ca ternary system [5], it should be possible to deoxidize even pure titanium by PESR using "active slags" where metallic calcium is added to the flux as deoxidation agent. The basic principle of Ti/Ti-alloy deoxidation by Ca (Fig. 3) is based on the reaction between oxygen dissolved in the metal phase as TiO with calcium dissolved in the slag which results in precipitation of CaO according to Eq. (1).

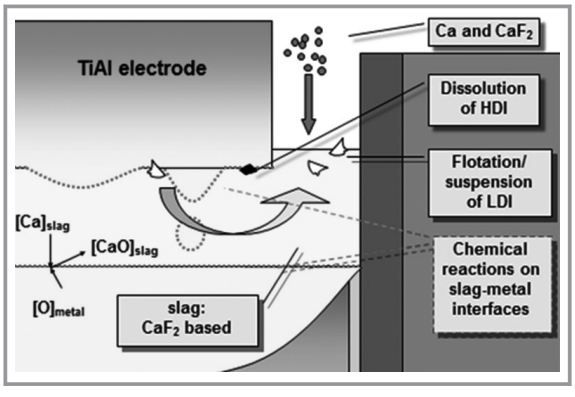

Figure 3. PESR deoxidation of TiAl.

As a main characteristic of the ESR process only a partial volume of the total metal is in the molten state at any time of the process and backmixing is limited to this volume. Thus, the major challenge during pressure electroslag remelting (PESR) deoxidation of titanium is to achieve a homogeneous oxygen distribution with respect to the full length of an ingot. Since the slag enriches in CaO during the melt and is being depleted in calcium, this will naturally lead to a shift of the thermochemical equilibrium to the left side of Eq. (1) and therefore decreases the deoxidation effect. As a consequence, the oxygen distribution would vary over the ingot height. Considering the law of mass-action and assuming constant temperatures and concentrations with fixed activities of TiO and Ti (by alloy specifications), it becomes obvious that a constant ratio f according to Eq. (4) throughout the whole melting time is key to a successful deoxidation procedure. Therefore, the activity of calcium has to be continuously increased with rising CaO concentrations in the slag during the process for compensation. Furthermore, the activity of CaO can be decreased by diluting via charging of CaF_2 to the slag [12].

$$f = \frac{a(\mathrm{CaO_{slag}})}{a(\mathrm{Ca_{slag}})} \equiv \text{const.} \tag{4}$$

Final refining of TiAl alloys can be achieved by VAR. Well known metallurgical advantages of the Ti-VAR process are vacuum refining (e.g., Mg distillation from Ti sponge and hydrogen degassing) and production of structurally homogenous and substantially macro segregation free metal. VAR offers excellent metallic cleanness due to the removal of small non-metallic inclusions (NMI), mainly by flotation effects. In the presented case, due to the sufficiently high Ca vapor pressure, Ca distillation according to Eq. (5) from TiAl is possible by VAR. Even at low metal pool temperatures, Ca contents less than 40 ppm are thermochemical possible at 5 Pa pressure (Fig. 4).

$$(\mathrm{Ca})_{\mathrm{TiAl}} = \{\mathrm{Ca}\} \tag{5}$$

with [ ] being dissolved, and { } being vapor compounds.

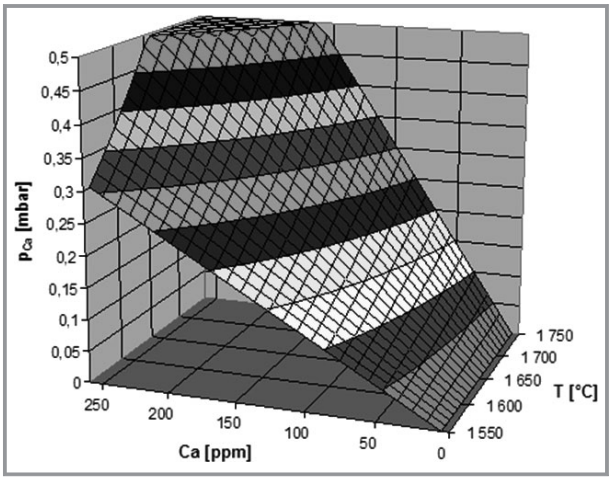

Figure 4. Vapor pressure of Ca according to VAR pool temperature and Ca content in γ-TiAl (FactSage; data: ELEM with $\gamma Ca = 1$).

 © 2015 WILEY-VCH Verlag GmbH & Co. KGaA, Weinheim

2.2 Investment Casting

Investment casting belongs to the group of lost form casting as the original pattern and mold are destroyed after casting. Complex and thin-shaped components can be produced with a minimal post processing since the surface quality is at very high level. Therefore, this casting technology is suitable for production of net-shape or near net-shape cast parts [13 – 14].

The investment casting process can be divided into different steps. Fig. 5 shows the process chain of the shell mold manufacturing, materials procurement, followed by casting. The first step is the preparation of the base material as ingots. Even small variations in alloy composition or heterogeneous microstructures can have a significant impact on the characteristics and reproducibility of the cast parts. Therefore, the tolerances of alloying elements for TiAl alloys are typically lower than ±0.5 at % [15 – 16].

The next step is the manufacturing of the wax patterns. The patterns are typically produced by injection of wax into a metallic die. In the metallic die all dimensional changes such as contractions of the wax, the metal and the ceramic mold are considered. Subsequently the wax patterns are assembled into a cluster to increase the economic feasibility of the process. The design of the wax cluster is based on empirical as well as numerical simulation data [17]. By dipping the wax clusters into ceramic slurries (a mass containing refractory powder and binders) adhered with refractory sand, a layer of the shell mold is formed.

The ceramic mold is built up by repeated dipping and sanding steps. Due to the high reactivity of TiAl alloys a combination of yttria (Y_2O_3) for the front layers and aluminum oxide (Al_2O_3) has been proven to be useful. After removing the wax from the mold in a steam autoclave, the mold is fired at high temperature to receive the final strength [18].

The casting process itself combines the shell mold and the ingot production and is carried out under vacuum, wherein the melting is usually done by a vacuum arc remelting (VAR), plasma arc melting (PAM) or induction skull melting (ISM). For casting of net shape or near net-shape components, a pressure-assisted casting process such as the centrifugal casting process is used. In the further steps the ceramic shell is removed and the cast parts are separated from the cluster by a water jet cutter [17, 19 – 21].

3 Experimental Work

3.1 Feedstock Material

Scrap produced during investment casting that meets the specifications of the alloy GE4822 was provided by ACCESS as feedstock material. The material was analyzed randomly by ICP-OES (inductively coupled plasma optical emission spectrometry) and CGHE (carrier gas hot extraction) to determine the exact chemical composition. The results are shown in Tab. 2. To compensate any material losses that may occur during the recycling process, primary alloying elements may also be used. Due to the high melting point of niobium, a Nb-Cr-Al master alloy is preferred.

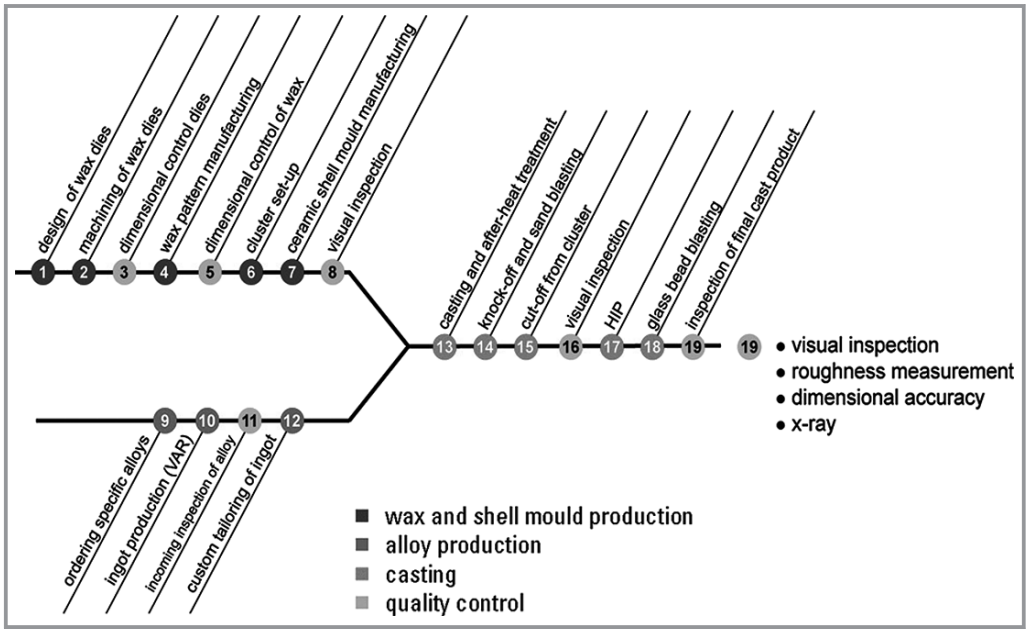

Figure 5. Process steps of investment casting process as developed for qualifying a process route for TiAl components [21].

 © 2015 WILEY-VCH Verlag GmbH & Co. KGaA, Weinheim

Table 2. Random analysis of investment casting scrap material.

Sample	Chemical composition [wt %]						
	Ti	Al	Nb	Cr	Fe	C	O_2
A-1	59.506	32.296	4.934	2.444	0.105	0.003	0.0515
A-2	59.218	32.620	4.989	2.452	0.047	0.003	0.1318
A-3	59.184	32.348	5.154	2.526	0.038	0.005	0.0746
Average	59.303	32.421	5.026	2.474	0.063	0.004	0.0860

3.2 Vacuum Induction Melting

3.2.1 Experimental Setup

The consolidation investigations were performed in one of IME's vacuum induction furnaces (PVA VSG 100) with a maximum melting power of 150 kW and a frequency of 2 kHz. The furnace chamber possesses a volume of 1090 L and can be evacuated to a pressure of 10^{-3} mbar. Therefore, a gate valve vacuum pump and a roots pump are available. Crucibles with a maximum volume of 14 L and CaO as crucible material were used. The pouring takes place in a water cooled copper mold using a pouring cup and a pouring nozzle. Both the pouring cup and the pouring nozzle have been coated with an Y_2O_3 coating to prevent reactions with the melt (Fig. 6). Furthermore, the pouring cup can be preheated to up to 800 °C.

Figure 6. Vacuum induction furnace PVA VSG 100 with prepared CaO crucible. The pouring nozzle as well as the pouring cup is Y_2O_3 coated.

3.2.2 Experimental Procedure

At the beginning of each vacuum induction melt approx. 26 kg of the feedstock material is charged into the crucible. After closing the furnace it is evacuated to a pressure of below $8.0 \cdot 10^{-2}$ mbar and backfilled with Ar to 500 mbar. To remove possible oxygen residues in the atmosphere the furnace is evacuated again to below $8.0 \cdot 10^{-2}$ mbar. The melting power is switched on and increased each 20 min to prevent cracks in the crucible. When almost 50 % of the maximum melting power is reached, the furnace is backfilled with Ar to a pressure of 650 mbar to prevent evaporations. After the feedstock material is molten the pouring cup is preheated and the melt is held at a temperature of 1560 °C for 10 min to obtain a good homogenization. Afterwards, the melt is tapped in a water cooled copper mold. After several hours of cooling time the ingot is stripped.

3.3 Ingot Bonding

To use the consolidated material in a subsequent pressure electroslag remelting process and perform a deoxidization, it is necessary to combine two ingots to one electrode by bonding. Due to the very strict specification, the ingots cannot be welded by using welding additives. Furthermore, due to the increased oxygen content in the material the electrodes become very brittle what makes an electrode beam welding difficult to implement. Therefore, a mechanical bonding by a native thread rod is realized (Fig. 7).

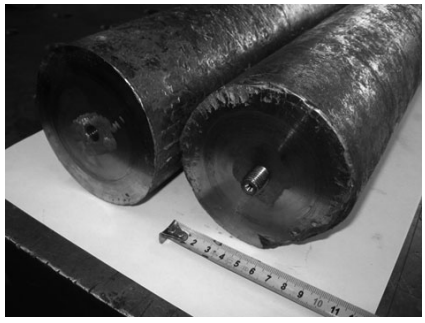

Figure 7. Mechanical bonding of two VIM ingots with a native thread rod.

3.4 Electroslag Remelting

3.4.1 Experimental Setup

The experiments were performed in the IME pressure electroslag remelting furnace (Fig. 8a) that is controlled by means of computer-aided software. The furnace is capable to remelt electrodes with a maximum diameter of 110 mm and a length of up to 1340 mm. Water-cooled copper molds with a height of up to 900 mm and a conical shaped inner diameter of about 170 mm are available. The remelting is performed in a chamber consisting of a closed system that can be used at atmospheric pressure or pressures up to 50 bars. The power supply is carried out by a thyristor control, where an operating voltage of 66.6 V and a current of 6 kA, 80 V and 5 kA can be tapped. Both cases result in a maximum power of approximately 400 kW.

3.4.2 Experimental Procedure

Before the furnace is closed, the electrode with a diameter of 105 mm and a length of around 1125 mm is connected to the electrode rod via titanium stub. A starting plate made of

 © 2015 WILEY-VCH Verlag GmbH & Co. KGaA, Weinheim

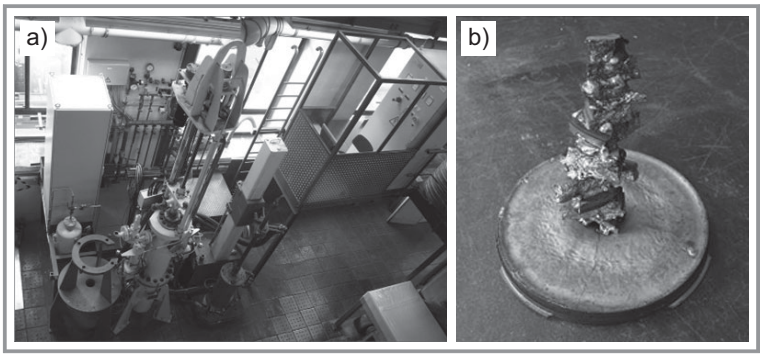

Figure 8. a) IME pressure electroslag remelting furnace with a remelting power of 400 kW and a process pressure of up to 50 bar; b) ESR starter turret made of Ti-50Al sputter targets.

Ti-50Al sputter targets (Fig. 8b) is placed on the crucible bottom to ensure electrical contact during the starting phase of the process.

Afterwards, the crucible is filled with 4.0 kg of process slag that consists of the technically pure CaF_2 slag Wacker Electrolux 2052 (> 97 wt % CaF_2) including 124 g of metallic calcium. The furnace is closed and, in order to avoid reactions with oxygen from ambient air, the vessel is evacuated to a pressure of 10^{-1} mbar. Consecutively, the vessel is backfilled with Ar gas to the desired process pressure of 20 bars to avoid excessive Ca evaporations.

3.5 Vacuum Arc Remelting

3.5.1 Experimental Setup

During the experiments, a IMEs vacuum arc remelting furnace ALD VAR L 200 with a melting power of up to 300 kW is used and which is controlled by means of a computer-aided software. The furnace has a melting capacity of around 180 kg of steel while electrodes with a maximum length of 1140 mm can be used. The remelting process takes place in water cooled copper crucibles with a diameter of 120, 160 or 200 mm while the vessel can be evacuated to a pressure of 10^{-5} mbar. Therefore, a gate valve vacuum pump, a roots pump as well as an oil diffusion booster pump are available.

3.5.2 Experimental Procedure

As feedstock material two PESR ingots are connected to one electrode via native rod (see Sect. 3.3). The electrode is put into the furnace and some native grindings are placed on the bottom of the crucible to simplify the start of the process. Analog to the previous PESR process, the VAR process consist of a starting phase, a melting phase and a hot topping. In the starting phase, the power is raised slowly while the native grindings prevent a contamination of the metal with copper from the crucible bottom plate. After the starting phase a steady melting phase is performed in which Ca residues and possible non-metallic inclusions are removed. After performing a hot topping phase the process stops.

3.6 Investment Casting

The quality of the ingot was verified by the investment casting process. For this purpose a cluster of six low pressure turbine blades (LPTB) has been prepared and cast. The six blades were assembled by wax soldering around a central melt distributor on top to build up a cluster for manufacture of the ceramic shell mold. The cluster consists of a central rod and a gating system at the bottom as connection between the blades and the central rod for stability issues. From the wax cluster the shell mold was made by usual dipping and sanding processes. The shell mold consists of front layers made from Y_2O_3 and several back-up layers based on Al_2O_3. After autoclaving and de-bindering the shell molds were fired according to the ACCESS standard procedure.

The casting of the blades was performed by centrifugal investment casting using the Leicomelt TP 5 centrifugal caster available at ACCESS. In the Leicomelt caster the melting of the alloy is performed by induction skull melting (ISM) in a 2 L water-cooled copper crucible with a melting power of up to 600 kW. After melting and a minimum holding time the melt is cast under vacuum in the preheated ceramic shell molds spinning with the predefined rotation speed. The process relevant parameters are listed in Tab. 3.

Table 3. Process parameters of Leicomelt TP 5 centrifugal caster.

Parameter	Value
Mold temperature [°C]	1100
Rotation speed [rpm]	200
Vacuum [mbar]	0.1
Casting temperature [°C]	1620
Process duration [min]	max. 15

After de-molding, the blades were hot isostatic pressed (HIP) according to aerospace specifications in order to close internal micro porosity. HIP is usually performed at elevated temperatures between 1100 – 1200 °C and high pressure between 160 – 180 MPa. Subsequently, all blades were heat treated according to aerospace specifications in order to develop a fully lamellar microstructure. For characterization of the texture one blade was cut and prepared by grinding, polishing and etching by Kroll's reagent for metallographic analysis. Characteristic images were taken under 100× magnification.

 © 2015 WILEY-VCH Verlag GmbH & Co. KGaA, Weinheim

4 Discussion

After investment casting residuals of ceramic shell molds can be found in the scrap. To avoid a contamination with yttrium and silicon, the feedstock has to be cleaned properly. Furthermore, the feedstock analysis showed slight deviations to the GE4822 specifications. Therefore and because of material losses that may occur during the melting campaign, the feedstock composition has to be adjusted by using a mixture of scrap material and virgin material. As forecasted, during VIM a reaction between the CaO crucible and the melt takes place. This reaction results in a slight oxygen pickup of around 400 ppm ending up with an oxygen content of around 1100 ppm. Since previous experiments have shown oxygen pickups of 5000 ppm while using alumina crucibles, CaO crucibles show very good thermochemical stability and are preferred. The low oxygen pickup is also reflected in the calcium intake. With regard to Fig. 2, calcium contents of 400 – 1400 ppm are expected depending on the temperature. The analysis shows a calcium content of around 400 ppm, confirming that even with low melting times the thermochemical equilibrium is reached. Therefore, it can be stated that the amount of oxygen and calcium pickup depends heavily on the crucible material and the temperature, which is why most stable crucible materials and low melting temperatures are preferred.

Depending on the oxygen content of the VIM ingots the amount of metallic calcium that is added to the process during PESR melting phase has to be chosen carefully. Since the oxygen content influences the mechanical treatment, the oxygen content must be set accurately. Therefore, the full chemical analysis of the electrodes and a thermochemical model to predict the necessary amount of calcium is indispensable. The oxygen content can be set accurately to values of 200 – 1200 ppm. However, it should be noted that no thermochemical equilibrium of Ca and O is reached. Therefore, it must be assumed that due to the high remelting temperatures during PESR, calcium evaporations are favored. As a consequence, only small amounts of calcium have to be removed by VAR, on the other hand, higher amounts of deoxidant have to be used. Concerning contaminations that are traceable to the slag like fluorine, no impact has been observed. However, due to the formation of a slag skin on the PESR ingot, the ingot has to be grinded to prevent carrying slag to the VAR process.

Since calcium residues will evaporate and condense at the furnace walls during investment casting, the calcium content has to be reduced during VAR. The experiments have shown that a high melting power in combination with a low pressure should be chosen to boost calcium evaporations. It must be ensured that this also boosts aluminum losses, which has to be considered during feedstock weighing.

The analysis results of a recycling ingot (50 % scrap / 50 % virgin material) are shown in Tab. 4. It can be seen that the recycling process was successful and that the average composition is within the specifications. There is only minor excess of "Others" which might be explained due to analysis tolerances.

During the melting and casting process no differences to primary titanium aluminide alloy could be found. Fig. 9

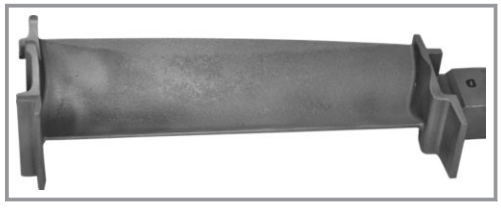

Figure 9. Investment casted LPT blade of secondary GE4822 alloy (50 % scrap / 50 % virgin material).

Table 4. Analysis results of a recycling ingot after VIM-PESR-VAR.

Sample	Chemical composition [wt %]											
	Ti	Al	Nb	Cr	Fe	Y	Ca	C	O	N	H	Other
E-01	59.05	33.21	4.79	2.58	0.025	0.034	0.004	0.015	0.101	0.037	0.004	0.059
E-02	58.91	33.12	4.83	2.56	0.212	0.032	0.003	0.015	0.158	0.026	0.004	0.059
E-03	59.06	33.20	4.89	2.56	0.013	0.031	0.001	0.013	0.109	0.008	0.003	0.058
E-04	58.95	33.18	4.90	2.68	0.072	0.035	0.005	0.012	0.104	0.014	0.004	0.087
E-05	59.09	33.09	5.00	2.56	0.013	0.029	0.004	0.015	0.119	0.021	0.004	0.087
E-06	58.64	33.51	4.93	2.74	0.056	0.031	0.003	0.009	0.143	0.025	0.004	0.078
E-07	59.17	33.07	4.92	2.58	0.006	0.038	0.003	0.011	0.100	0.014	0.004	0.095
E-08	59.31	32.94	4.90	2.47	0.005	0.027	0.002	0.012	0.092	0.023	0.004	0.093
E-09	58.68	33.66	4.96	2.63	0.017	0.030	0.003	0.011	0.100	0.014	0.004	0.089
E-10	59.06	33.23	4.85	2.55	0.008	0.033	0.003	0.011	0.108	0.016	0.004	0.095
Average	58.99	33.22	4.90	2.59	0.043	0.032	0.003	0.012	0.113	0.020	0.004	0.080

 © 2015 WILEY-VCH Verlag GmbH & Co. KGaA, Weinheim

shows an investment casted blade from recycled ingot material. The images of the microstructure of the cast part after HIP and heat treatment are shown in Fig. 10. The metallographic analysis of the microstructure shows the typical duplex structure for the GE4822 alloy. Since the microstructure is mainly responsible for the mechanical properties, it can be assumed, that the material shows typical values for elasticity modulus and creep resistance.

5 Conclusion

Due to material losses during the recycling process (splashes during VIM, evaporations during ESR and VAR) the exclusive use of scrap material is not advisable and will results in a deviation to the specifications. Nevertheless, by identifying weak spots of the process and an accurate adjustment of the process parameters homogeneous ingots within the specifications consisting of up to 50 % recycling material can be produced. After investment casting, this secondary alloy possesses a duplex microstructure. Hence, it can be assumed that the mechanical properties of secondary alloys show no significant deviations from primary alloys.

Thus, it can be stated that the recycling process is a reasonably priced, reproducible process that provides material within the required specifications. Therefore, the IME process shows extremely high potential to become state of the art in titaniumaluminide recycling for aviation applications.

The studies described in this paper were performed for the four year project E-BREAK funded by the Seventh Framework Program of the European Commission under grant agreement n° 314366. The authors want to express their gratitude to the European Commission for this financial support.

Abbreviations

BTF	buy-to-fly
CGHE	carrier gas hot extraction
ESR	electroslag remelting
HIP	hot isostatic pressing
IC	investment casting
ICP-OES	inductively coupled plasma optical emission spectrometry
ISM	induction skull melting
LPTB	low pressure turbine blade
NMI	non-metallic inclusion
PAM	plasma arc melting
PESR	pressure electroslag remelting
RPK	revenue passenger kilometers
VAR	vacuum arc remelting
VIM	vacuum induction melting

References

[1] H. Clemens, *BHM* **2008**, *153*, 337 – 341. DOI: 10.1007/s00501-008-0396-z
[2] S. Knippscher, Frommeyer, *Materialswiss. Werkstofftech.* **2006**, *37*, 724 – 730. DOI: 10.1002/mawe.200600067
[3] E. A. Loria, *Intermetallics* **2001**, *9*, 997 – 1001. DOI: 10.1016/S0966-9795(01)00064-4
[4] J. E. Barnes, W. Peter, C. A. Blue, *Mater. Sci. Forum* **2009**, *618 – 619*, 165 – 168. DOI: 10.4028/www.scientific.net/MSF.618-619.165
[5] J.-C. Stoephasius, B. Friedrich, *Adv. Eng. Mater.* **2007**, *9*, 246 – 252. DOI: 10.1002/adem.200700009
[6] C. Lochbichler, B. Friedrich, G. Jarczyk, *Adv. Mater. Sci.* **2007**, *7*, 81 – 88. DOI: 10.2478/v10077-008-0009-2
[7] J. Reitz, C. Lochbichler, B. Friedrich, *Intermetallics* **2011**, *19*, 762 – 768. DOI: 10.1016/j.intermet.2010.11.015
[8] J. L. Murray, H. A. Wriedt, *Bull. Alloy Phase Diagrams* **1987**, *8*, 148 – 165.
[9] Y. Kobayashi, F. Tsukihashi, *Metall. Mater. Trans. B* **1998**, *29*, 1037 – 1042. DOI: 10.1007/s11663-998-0072-4
[10] F. Tsukihashi, E. Tawara, T. Hatta, *Metall. Mater. Trans. B* **1996**, *27*, 967 – 972. DOI: 10.1007/s11663-996-0010-2

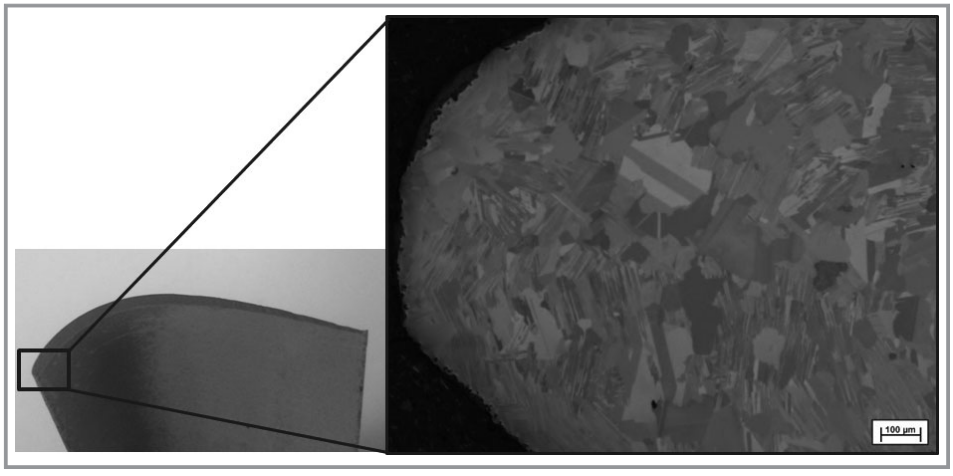

Figure 10. Metallographic cut of a low pressure turbine blade. A duplex microstructure was achieved after HIP and HT.

 © 2015 WILEY-VCH Verlag GmbH & Co. KGaA, Weinheim

[11] R. Nafziger, in *Proc. of the 2nd Int. Symp. on Electroslag Remelting Technology* (Ed: G. K. Bhat), Mellon Institute, Pittsburgh **1969**.
[12] J. Stoephasius, *Ph.D. Thesis*, RWTH Aachen University **2006**.
[13] H. Aue, W. Blank, F. Feikus, *Feinguss – Herstellung, Eigenschaften, Anwendung*, Bundesverband der Deutschen Gießerei-Industrie, Düsseldorf **2008**.
[14] E. Brunhuber, S. Hasse, *Giesserei Lexikon*, 16th ed., Fachverlag Schiele & Schoen, Berlin **2001**.
[15] F. Appel, J. D. H. Paul, M. Oehring, *Gamma Titanium Aluminide Alloys: Science and Technology*, Wiley-VCH, Weinheim **2011**.
[16] A. Lasalmonie, *Intermetallics* **2006**, *14*, 1123 – 1129. DOI: 10.1016/j.intermet.2006.01.064
[17] A. Choudhury, M. Blum, *Vacuum* **1996**, *47*, 829 – 831. DOI: 10.1016/0042-207X(96)00076-0
[18] O. Kättlitz, *Ph.D. Thesis*, RWTH Aachen University **2014**.
[19] H. Kestler, H. Clemens, *Titan und Titanlegierungen: Herstellung, Verarbeitung und Anwendungen von Gamma TiAl-Basislegierungen*, Wiley-VCH, Weinheim **2002**.
[20] H. Nicolai, C. Liesner, *Titan und Titanlegierungen: Feinguss von Titan*, Wiley-VCH, Weinheim **2002**.
[21] J. Aguilar, A. Schievenbusch, O. Kättlitz, *Intermetallics* **2011**, *19*, 757 – 791. DOI: 10.1016/j.intermet.2010.11.014

 © 2015 WILEY-VCH Verlag GmbH & Co. KGaA, Weinheim